

Preprocessing Algorithms of Vision Research Damage to Concrete Railway Sleepers

Piotr LESIAK¹, Aleksander SOKOŁOWSKI²

Summary

The paper presents algorithms for the preprocessing of the visual method of detecting damages of concrete railway sleepers. It starts with acquiring images of the surface of the sleepers, by selecting the recorded frames of the images. Then, the color image is transformed into monochrome, so as to obtain the highest contrast possible. The Kanan and Cottrell algorithms were used for this purpose. A simple way is to segment the damage images of the sleepers, by thresholding, in order to binarize them. However, more elaborate algorithms are recommended. For this purpose, images are denoted using a median filter and further morphological operations to extract the edge of damage. For this purpose, noise is removed from images using a median filter, and morphological operations are carried out, to extract the edge of damage. In addition, texture images of the surface of the sleepers are used, removing them from the visual content. As the criterion for selecting the preprocessing algorithm, the shape of the image histogram and its standard deviation were assumed. Such prepared images form the basis for further assessment of the size of damages (cracks and voids) and classification of concrete sleepers.

Keywords: railway track, concrete sleeper, image processing algorithms

1. Introduction

Automated diagnostic systems of the railway track, improving the quality of inspections and reducing their time-consumption are the subject of interest of railway administrations all over the world. Automated diagnostic systems of the railway track, improving the quality of inspections and reducing their time-consumption are the subject of interest of railway administrations all over the world [7]. This applies to, among others diagnose railroad sleepers, the faults of which

can lead to the derailment of trains. This is particularly important in high-speed railways.

Previous work carried out in the country by a co-author of this paper was limited to wooden sleepers, in which the nature of cracks is usually regular, along the growth rings wood [2, 3, 4] and [16].

Faults in concrete sleepers (prestressed concretes) have a completely different character [9, 11]. As a rule, they are irregular, (Fig.1).

In the paper [8], such damages were reviewed and the factors underlying their formation were ana-

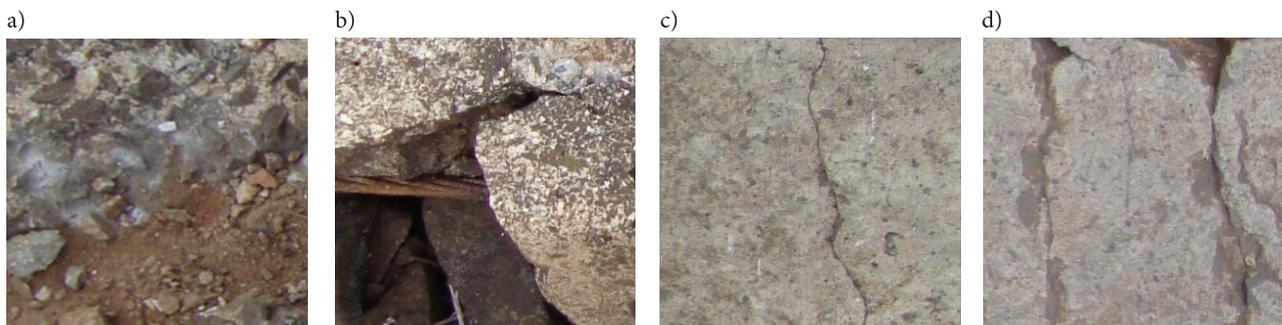


Fig. 1. Examples of faults to concrete sleepers: a) loss, b) loss, with visible reinforcement of concrete, c) crack, d) double crack [photo. authors]

¹ Ph.D. D.Sc. Eng.; University of Economics and Innovation in Lublin, Faculty of Transport and Computer Science; e-mail: piotr.lesiak@wsei.lublin.pl

² Ph.D.; Rzeszow University of Technology, Department of Management; e-mail: alex5@prz.edu.pl.

lyzed [19]. The influence of static and dynamic loads on stress and cracking of compressed concrete sleepers was also evaluated [13, 21]. Mechanics of their cracking are also described by investigating the size of cracks [18], as well as by freezing water in them [20]. However, in [10] the results of tests showing the destruction of concrete sleepers, caused by vibrations above 100 Hz, were presented.

All these studies, consequently, were to answer the questions which factors and to what extent they affect the operational damage of concrete foundations (cracks, defects, chips, etc.).

On the other hand, the target aim of the authors is to diagnose these damages. Various research techniques are used here, in which the latest one, using acoustic emission, can be distinguished [5].

The basic method implemented recently in the mobile diagnostics of the track is the vision method. As a rule, it is introduced to automate it, also when detecting damage to railway sleepers [1] and [17]. In more detailed considerations, automatic selection and classification of damages of concrete sleepers is carried out, including three main stages: pre-processing, detection of damaged foundation and detection of damage itself [6].

In commercial solutions, such a system will be used in Poland by the Diagnostic Center PKP PLK SA. This goal will be served by a measuring railcar with the symbol DP560, in which the measurement systems were developed by the Italian company MerMec. The Polish company Graw Sp. z o.o. has installed on the TMS tamping system a video monitoring system for the Dutch railways, one of which is the inspection of sleepers [information accessed at PKP PLK S.A. Centre of Diagnostics].

Evaluation of damage images of sleepers requires their initial preparation, for which preprocessing operations are used [2, 16]. They will be the subject of the authors' deliberations.

Preprocessing operations eliminate variables that do not provide relevant information, and the ranges of these variables significantly differ from each other. As a result of this processing, the characteristic features of the foundation image are automatically extracted, in this case its cracks and voids. This is not an easy issue, due to numerous disturbances, including those introduced by railway ballast, vegetation and other various objects lying on the tracks, as well as variable texture. Not all disturbances are possible to be removed at this stage of consideration, so they were left for further research. The proposed algorithms use images of sleepers, not disturbed by rail gravel.

2. Preprocessing algorithms

In the proposed preprocessing method, the first step is to transform the color image of concrete foundations into a monochrome image. In the color

theory, saturation or chromaticity is the subjective intensity of the color. The intensity values of the color components of the image at 8-bit resolution are in the range from 0 to 255, i.e. [15]:

$$C_{RGB} = (R(i, j), G(i, j), B(i, j)) \quad (1)$$

where C_{RGB} is the intensity of the color of the color image in the pixel i, j , while R, G, B is the intensity of the individual component colors.

In RGB space, saturation is understood as the Euclidean distance of a given color, from a gray point with the same brightness as the color considered.

In order to transform the images of the sleepers, one can use the chosen from numerous Kanan and Cottrell algorithms [14]:

$$Gr(i, j) = 0.299 R(i, j) + 0.587 G(i, j) + 0.114 B(i, j), \quad (2)$$

where $Gr(i, j)$ is the brightness of the gray monochrome image in pixel i, j . Fig. 2 gives an example of the functioning of these algorithm.

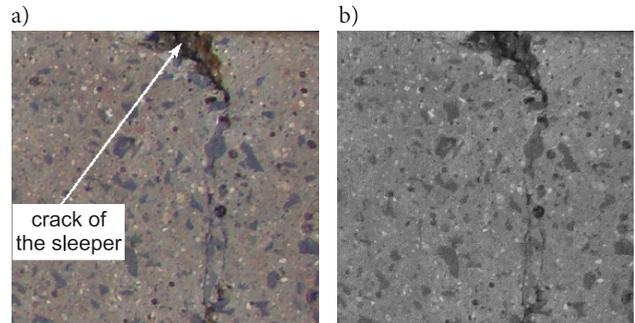


Fig. 2. Illustration of the processing of a fragment of a visual image of a concrete foundation with a concrete crack: a) colorful input image, b) the monochrome version of the image according to the algorithm described by the formula (2) [photo. authors]

Then, cross-sections of the image brightness waveforms along horizontal and vertical monochrome image paths are set, positioned in the area of the largest damage, as in Fig.3a. A significant effect of the concrete texture is visible here.

In turn, the image from Fig. 3a was segmented by thresholding [16]. This method can be called simplified. An important problem is the proper selection of the threshold value. The background image contains pixel values centered around two mean values, \bar{u}_1 – fault in the sleeper and its background \bar{u}_2 , i.e. the surrounding surface without fault, each with a Gaussian distribution, which were designated P_1 and P_2 respectively, with $P_1 + P_2 = 1$. For these assumptions, the threshold value T is determined, minimizing the total error of segmentation of the image, i.e. the number of pixels belonging to the background defect and counted to its background (false positive) and pixels

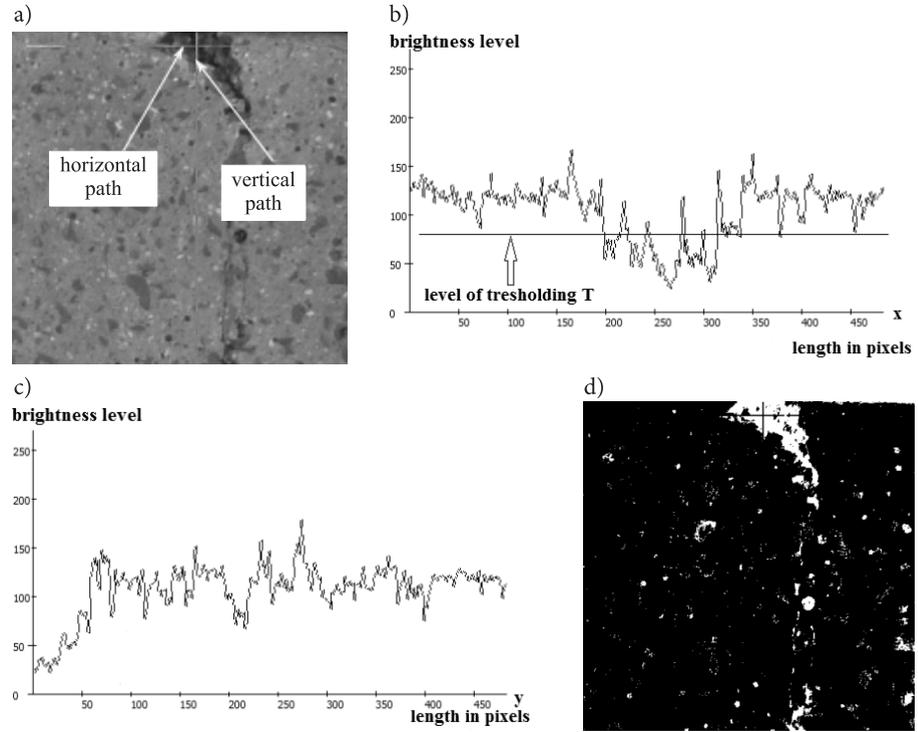


Fig. 3. Illustration of transformation of the image from the monochrome version – Fig. 3a to the binary version – Fig. 3d, where Fig. 3b represents changes in the brightness of the image along the horizontal line, while Fig. 3c represents changes in the brightness along the vertical line [own work]

belonging to the background of the fault and counted to its defect (false negative).

For equal variances σ^2 of the brightness distribution of the defect image and background of the railway sleeper, the threshold value minimizing the segmentation error is:

$$T = \frac{\bar{u}_1 + \bar{u}_2}{2} + \frac{\sigma^2}{\bar{u}_1 - \bar{u}_2} \ln \left(\frac{P_1}{P_2} \right) \quad (3)$$

For $P_1 = P_2$, the optimal segmentation threshold value is equal to the arithmetic mean of the mean brightness of the railway underlayer defect and its background.

As a result of using this procedure, a binarized image was obtained, Fig. 3d, i.e. represented in a two-color version (black and white). In this image, the largest white area was obtained, including the bursting of the railway sleeper and at the same time where there is no defect, the least white noise possible. So the image brightness values above the threshold are presented in black, and below – in white. It has its justification in the fact that by presenting a darker stain as white, and part of the railway foundation undamaged – with black color, having such a black and white image at hand, it is easier to determine the size of the damage.

This process is illustrated in Fig. 3b, where it can be seen in the form of a horizontal continuous line at

the level of threshold T . In this case, there is a rupture of the railway sleeper or very close to this condition.

Initial assessment of image quality is usually made based on its histogram. The narrow histogram is the poor image contrast and the difficulty of extracting information, Figure 4 and the associated low standard deviation:

$$\sigma_u = \sum_{l=0}^{L-1} (u_l - \bar{u})^2 h(u_l), \quad (4)$$

where:

- L – the total number of available image brightness levels in l , where $l = 0, \dots, L-1$ (for a typical 8-bit image of defect L is equal to 256),
- $h(u_l)$ – number of pixels of the underlay fault with brightness level u_l .

Such a situation applies to Fig. 3a, because the standard deviation, determined from formula (4), is $\sigma_u = 18$. This parameter will be the criterion for selecting the preprocessing method simplified by direct binarization, or complex method using more complex image processing. Here, the choice is unambiguous, because the image from Fig. 3d contains a series of point distortions, with at the same time a poorly shown crack in the bottom part. This leads to the use of additional image processing algorithms from Fig. 3a before segmentation.

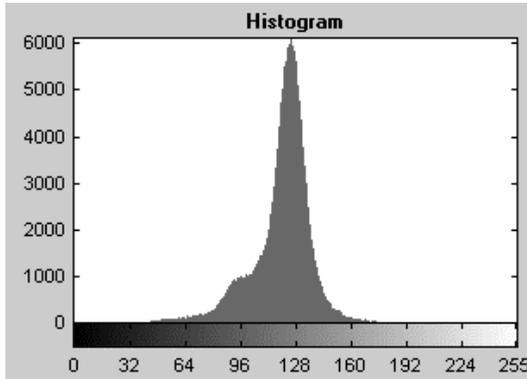


Fig. 4. Histogram of the image of a concrete sleeper with a crack as in Fig. 3a [own work]

The routine activity is usually denoise. An efficient method can be the use of nonlinear filtration with so-called order statistics [16]. For this case, a non-linear median filter was used, in which there is a possibility to choose the filter's action area, which is shown for the 10-pixel environment in Figure 5a. In contrast to direct binarization, there is a decrease in single point interference, which can be seen after comparing Fig. 5b and Fig. 3d. In turn, comfortable and quick morphological operations, *thin* and *dilatation* were applied, thanks to which there was a better extraction of the crack edges of

the fault. This is a relatively universal approach and works well with other faults.

A significant problem in such cases is small changes in the surface of the fault in the form of spot spatter formed in the process of production, assembly or exploitation, which usually do not carry the danger of enlargement. Their elimination from the image of the sleeper is associated with a significant blurring of large defects and, as a result, a reduction in their size, due to the use of other preprocessing operations.

The authors also attempted to eliminate from the image of the damaged sleeper its surface texture. Texture in the aspect of perception, can be associated with certain physical features, such as smoothness, roughness, regularity or directionality. Its presence in the vision images of the surface of the faults is obvious, where it is a background. It adopts different sizes of granularity and brightness amplitude, as shown in Fig. 6.

The experiments that were undertaken consisted in determining the difference between the image of the damaged sleeper and the texture constituting the background. Of course, both compared images should have the same size and geometric resolution, 400×400 pixels. In contrast, the quantization of the brightness amplitude had a 8 bit resolution, Fig. 6b and d. This operation consists in subtracting the pixel amplitude from each other with the same geometrical coordinates.

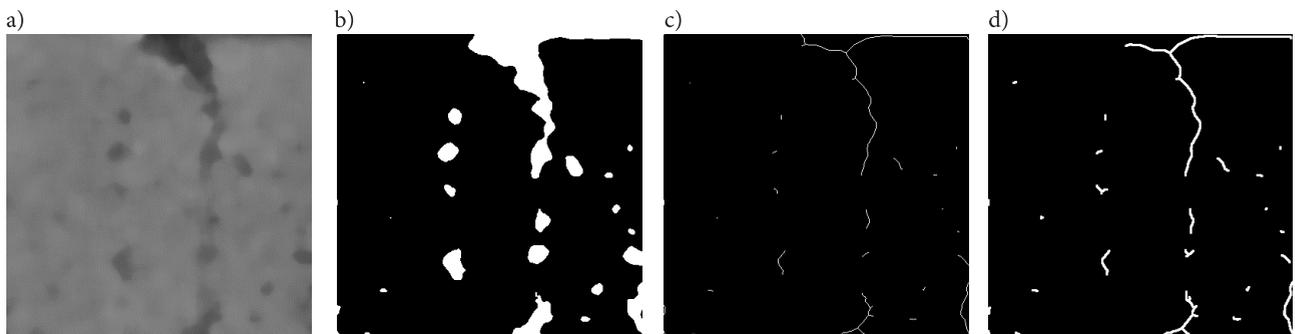


Fig. 5. Illustration of the subsequent phases of the image processing of the concrete foundation crack from Fig. 3a: a) after median filtration, b) after thresholding, c) after morphological operations of *thin*, d) after *dilatation* [own work]

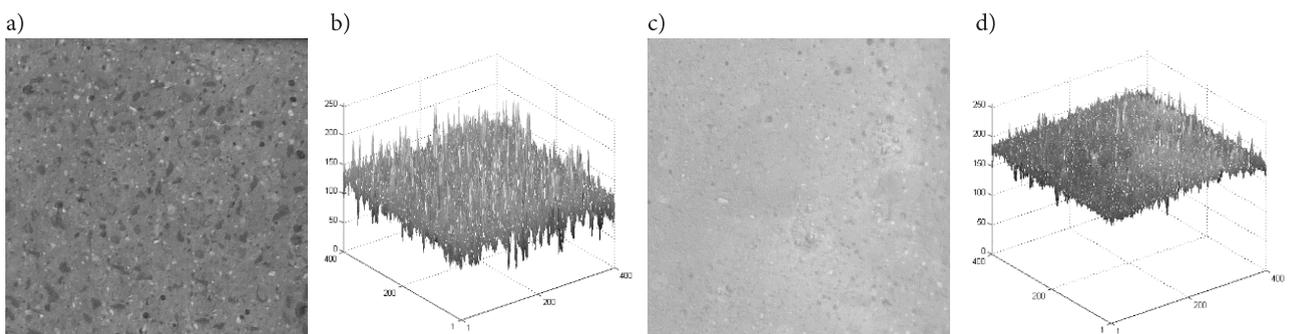


Fig. 6. Illustration of a surface texture of concrete sleepers: a) coarse surface of the sleeper in the range of medium brightness amplitude, b) image of surface quantized brightness amplitude from illustration a), c) fine-grained surface of the sleeper in the range of high brightness amplitude, d) image of surface quantized brightness amplitude from illustration c) [own work]

The same fracture image from Fig. 3a was used in the research. This is shown in Fig. 7. First, the difference between the crack image from Fig 3a and the concrete texture was determined, with similar graininess and brightness, as in Fig. 6a. The next processing operations were identical to Fig. 5. The resulting final image 7d does not differ much from the image from Fig. 5c, with the smallest single isolated noise disappearing as a result of eliminating its texture from the image. The correct choice of texture is obvious here,

the closest to the real one. In visual measurement systems, it should be recognized on the railway route.

3. Sample research results and their analysis

The criterion according to which the simplified or complex preprocessing algorithm is chosen is based on the standard deviation σ_u in the histogram. In the examples from Fig. 8, a simplified algorithm for im-

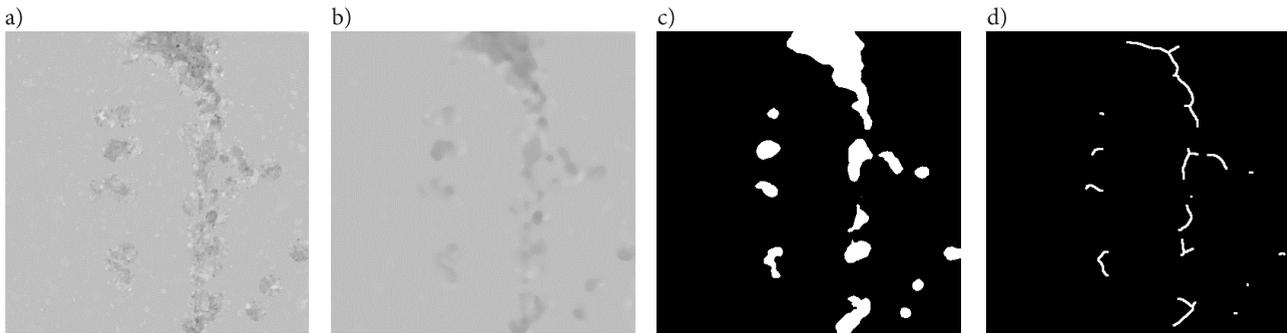


Fig. 7. Illustration of the subsequent phases of the image processing of the concrete sleeper crack from Fig.3a, where: a) is the difference of this image and the texture from Fig. 6, b) after median filtration, c) after thresholding, d) after morphological *thin* operations and *dilatation* [own work]

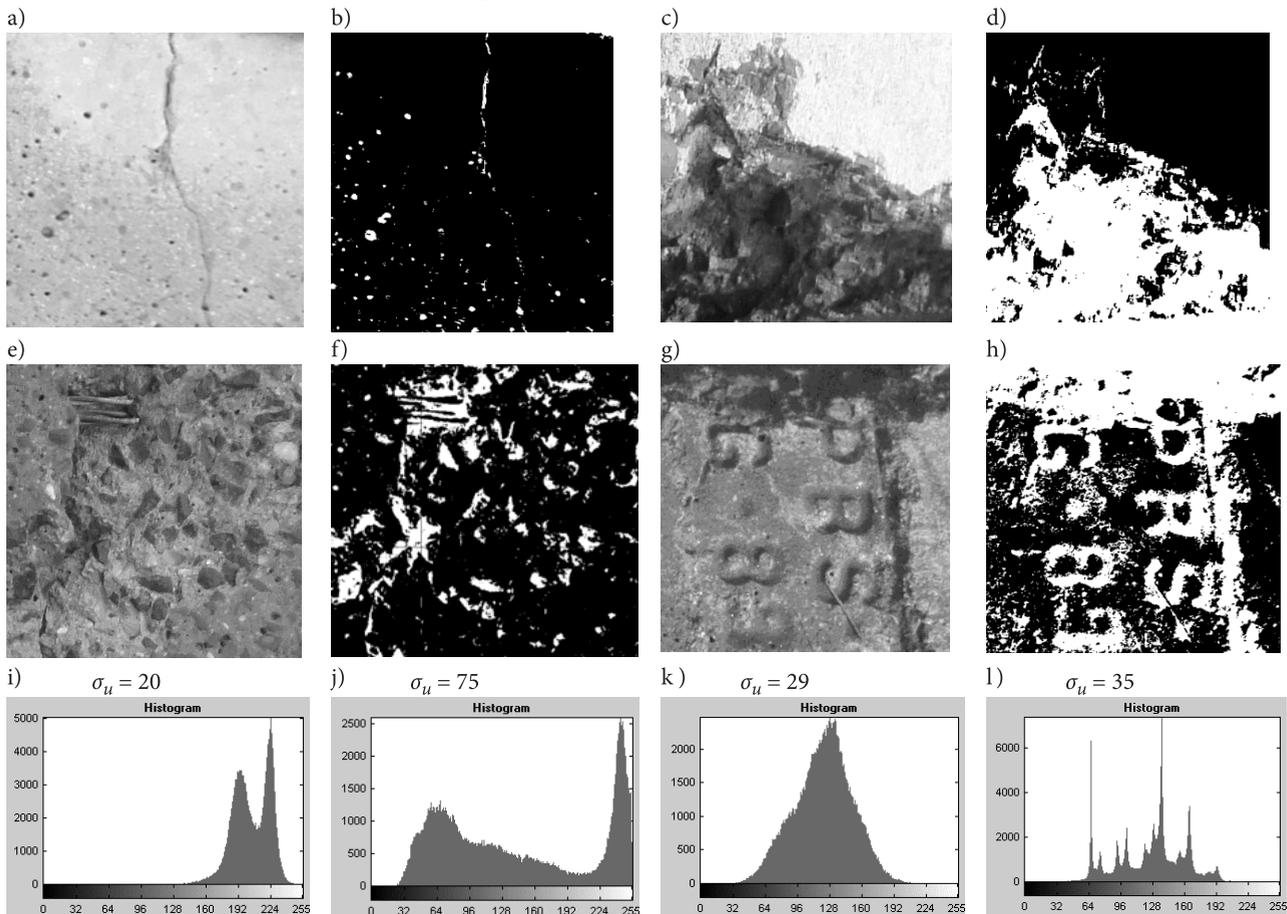


Fig. 8. Examples of image processing for concrete sleepers with several types of damage, their binarized form and histograms: a) and b) cracking sleeper, c) and d) – loss of sleeper, e) and f) – loss of sleeper with inferior lighting, g) and h) fragment of the description of the marking of the railway sleeper, i), j), k) and l) histograms of images from a), c), e) and g) respectively [own work]

age processing of concrete sleepers was applied. Thus, Figures 8a and b show the same crack of the sleeper, with the gray scale image from Fig. 8a being the effect of using formula (2). By choosing the appropriate level of thresholding, a continuous line will be obtained near the vertical path that determines the distribution of the brightness of the image. In this case, it can talk about a poor quality of the crack image, after applying this algorithm. The threshold level has been set to 155 if it takes 255 as the maximum brightness. At the lower level of thresholding, the image contains less information and the defect is worse or not at all visible. At the higher level of thresholding, the image shows interference from the spot irregularities of the sleeper. This is confirmed by the histogram from Fig. 8i, and the low value of its standard deviation $\sigma_u = 20$, which corresponds to the image from Fig. 8a, clearly indicating the need to choose a combination algorithm.

Figures 8c and d show the loss of sleeper. In contrast to the previous example, the binarized image shows a distinct loss, occupying about half the surface area. It can be said here that this is the best example of how the method works. The level of thresholding is equal to 110, if the lower the image is not continuous. This justifies the best stretched shape of the histogram from Fig. 8j and its high standard deviation $\sigma_u = 75$, because the image is contrasting. The simplified algorithm is fully justified here.

Images from Figures 8e and f also show the loss of the sleeper, similar in nature to that of previous figures 8c and d. Fig. 8f is less clear than figure 8d, this is due to the fact that its contrast is clearly lower.

This is confirmed by the relatively narrow histogram from Fig. 8g and low $\sigma_u = 29$. The threshold level is equal to 90. The image is not continuous, but gives the impression of covering the entire defect. It seems that changing the lighting conditions would improve its quality. Under these conditions, it is necessary to use a complex algorithm, extended to other processing functions than those presented in this paper. Figures 8g and 8h show what the image of an undamaged marked sleeper labeled with embossing. The marks placed on the upper surface of the sleeper should have a height of not less than 18 mm and a width of 5 mm, and be embossed in concrete to a depth of at least 3 mm. They contain the type of sleeper and rails, the year of manufacture (the last two digits), and the producer's mark [12]. It can be seen that it was a very old sleeper, because from 1989, despite this, the inscription has been clearly readable both before and after the binarization. A fairly broad spectrum with differentiated amplitude, Fig. 8h, is the result of imperfect lighting.

4. Conclusions

The paper presents the methods of preparing, i.e. preprocessing of visual images of concrete railway

sleepers containing faults, in order to further evaluate and classify them. Different ways to solve this problem have been proposed, along with analysis. First, the color image is transformed into monochrome. In the simplified method, faults are segmented, through the optimal choice of thresholding brightness of images, obtaining a binary image (black and white), with a defect in white. This is the starting point for further assessment and classification of damage.

The method seems to work correctly, but some improvements are needed. First of all, it should be specified which lighting will be the best, so that the area of damage can be accurately extracted from the image. In the experiments, the authors used photos taken manually with a fixed frame, with natural lighting. Therefore, in some cases it is difficult to obtain good conditions for damage exposure, especially at low contrast. This problem should be minimized in automated mobile measurement systems.

A complex algorithm, using several operations on images, will be particularly useful in numerous surface disturbances, such as local unevenness, punctuation cavities, greater granularity of concrete, especially in older products. The optimal solution would be to develop a permanent algorithm, regardless of the nature of the damage that could work in real time. In case of doubts, as is the case in the diagnosis of railway rail faults, the operator should be equipped with additional IT tools clarifying the final decision.

Therefore, the solutions proposed in the work should be developed and improved on the basis of good quality research samples.

In the next stage of visual inspection of concrete sleepers, after preprocessing, they are classified as "fit" and "not fit" for further use. Usually, for example, a neural network equipped with a component vector is involved: the number of cracks occurring in the classified undercoat, the length of the largest crack of the classified undercoat, the width of the largest crack of the classified undercoat, etc., what was the subject of the co-author's research in the case of wooden sleepers [3, 4]. However, the large variety of damage to concrete foundations makes the amount of samples necessary for analysis must be disproportionately larger.

Literature

1. Auglar, J., Lope, M., Torres, F., Blesa, A.: *Development of a stereo vision system for non-contact railway concrete sleepers measurement based in holographic optical elements*, Measurement 38, 22 June 2005, Elsevier, pp. 154–165.
2. Bojarczak, P., Lesiak, P.: *Preprocessing w diagnostyce wizyjnej podkładów kolejowych*, TransComp 2009, Logistyka 6/2009 (CD), s. 10.

3. Bojarczak P., Lesiak P.: *Application of neural networks into automatic visual diagnostic of railway wooden sleepers*, Międzynarodowa Konferencja Naukowa Transport XXI wieku, Białowieża 2010, Logistyka 4/2010 (CD), s. 10.
4. Bojarczak P., Lesiak P.: *Zastosowanie hybrydowej sieci neuronowej do klasyfikacji uszkodzeń drewnianych podkładów kolejowych*, Prace Naukowe, Transport, z. 78, Politechnika Warszawska, Warszawa 2011, pp. 23–36.
5. Clark A., Kaewunruen S., Janeliukstis R. and Papelias M.: *Damage detection in railway prestressed concrete sleepers using acoustic emission*, IMST 2017, IOP Conference, Series: Materials Science and Engineering 251, 012068, 2017 [online] <http://iopscience.iop.org/article/10.1088/1757-899X/251/1/012068/pdf> [access: 1 September 2018].
6. Delforouzi A., Tabatabaei A.H., Khan M.H., Grzegorzek M. A.: *Vision-Based method for automatic crack detection in railway sleepers*, In: Kurzynski M., Wozniak M., Burduk R. (eds) Proceedings of the 10th International Conference on Computer Recognition Systems CORES 2017. Advances in Intelligent Systems and Computing, Vol. 578. Springer, Cham 2018, pp 130–139.
7. Federal Railroad Administration, Office of Safety Analysis. Train Accidents by Type and Major Cause from Form: FRA F 6180.54. Jan.-Dec, 2004, April 6, 2005.
8. Ferdous W., Manalo A.: *Failures of mainline railway sleepers and suggested remedies – review of current practice*, Engineering Failure Analysis, Vol. 44, 2014.
9. Ferdous W., Manalo A., Aravinthan T., Remennikov A.: *Review of failures of railway sleepers and its consequences*, Proceedings of the first International Conference on Infrastructure Failures and Consequences 16-20 July 2014, RMIT University Melbourne, pp. 398-407.
10. Grassie S.L., Cox S.J.: The dynamic response of railway track with unsupported sleepers. Proceedings of the Institution of Mechanical Engineers, Vol.199, Part D, No. 2, 1985, pp.123–135.
11. Id-1. Warunki techniczne utrzymania nawierzchni na liniach kolejowych, PKP PLK S.A., Warszawa 2005.
12. Id-101. Warunki techniczne wykonania i odbioru podkładów i podrozdzielnic strunobetonowych, PKP PLK S.A., Warszawa 2010.
13. Jokūbaitis A., Valivonis J., Marčiukaitis G.: *Analysis of strain state and cracking of concrete sleepers*, Journal of Civil Engineering and Management, Vol. 22, 2016, pp. 564–572.
14. Kanan G., Cottrell G. W.: *Color-to-greyscale: does the method matter in image recognition?* PLoS ONE, Vol. 7, No 1, e29740, 2012, pp. 7-10, [online] <http://journals.plos.org/plosone/article?id=10.1371/journal.pone.0029740> [access: 1 September 2018].
15. Kumar T., Verma K.: *The theory based on conversion of RGB image to gray image*, – International Journal of Computer Applications, Vol. 7, No. 2, 2010, pp. 7–10.
16. Lesiak P., Bojarczak P.: *Przetwarzanie i analiza obrazów w wybranych badaniach defektoskopowych*, Monograficzna seria wydawnicza, Biblioteka Problemów Eksploatacji, Wydawnictwo Naukowe Instytutu Technologii Eksploatacji – PIB, Radom 2012, s. 185.
17. Ramesh S., Chavan S., Kankani J., Joshi U.: *Crack detection in concrete railway sleeper*, International Journal of Computer Sciences and Engineering, Vol. 04, Issue 02, 2016, pp. 142–144.
18. Rezaie F., Farnam S.M.: *Fracture mechanics analysis of pre-stressed concrete sleepers via investigating crack initiation length*, Engineering Failure Analysis, 58, Part 1, 2015, pp. 267–280.
19. Zakeri J.-A., Rezvani F.H.: Failures of railway concrete sleepers during service life. International Journal of Construction Engineering and Management 2012, 1(1), pp. 1–5.
20. Zi G., Moon D.Y., Lee S.-J., Jang S.Y. et.al.: *Investigation of a concrete railway sleeper failed by ice expansion*, Engineering Failure Analysis, 26, 2012, pp. 151–163.
21. You R., Li D., Ngamkhanong C., Janeliukstis R., Kaewunruen S.: *Fatigue life assessment method for prestressed concrete sleepers*, Frontiers in Built Environment, 15 Nov. 2017, [online] <https://www.frontiersin.org/articles/10.3389/fbuil.2017.00068/full> [access: 1 September 2018].